Neural control of motion-to-force transitions with the fingertip

Madhusudhan Venkadesan^{1,4} and Francisco J. Valero-Cuevas^{2,3,4}

¹Department of Mathematics, Cornell University, Ithaca, NY, USA

²Department of Biomedical Engineering, University of Southern California, Los Angeles, CA, USA

³Division of Biokinesiology & Physical Therapy, University of Southern California, Los Angeles, CA, USA

⁴Sibley School of Mechanical & Aerospace Engineering, Cornell University, Ithaca, NY, USA

Published in: Journal of Neuroscience, In Press

Address correspondence to:

Francisco J. Valero-Cuevas The University of Southern California 3710 McClintock Ave, RTH 404 Los Angeles, California 90089-2905

e-mail: valero@usc.edu Voice: 213.821.2084

New cell number: 323 428-0415

Fax: 213.821.3897

http://bme.usc.edu/valero/

Acknowledgements We thank R. V. McNamara III for technical support and experiment execution, F. A. Medina for EMG processing, Dr. V. J. Santos for help with study design, S. Song for machining and instrumentation, Drs. M. Price and S. Backus for fine-wire electrodes placement, and Drs. J. Guckenheimer, A. Ruina, M. Srinivasan, H. Lipson, K. J. Keenan, E. Todorov, and the anonymous reviewers for critical comments. This material is based upon work supported by the Whitaker Foundation (FVC), NSF Grants 0312271 & 0237258 (FVC), a NSF GRF (VJS), and NIH Grants AR050520 and AR052345 (FVC). Its contents are solely the responsibility of the authors and do not necessarily represent the official views of the National Institute of Arthritis and Musculoskeletal and Skin Diseases (NIAMS), the National Institute of Childhood and Human Development (NICHD), the NIH, the Whitaker Foundation or the NSF.

The neural control of tasks such as rapid acquisition of precision pinch remains unknown. Therefore, we investigated the neural control of finger musculature when the index fingertip abruptly transitions from motion to static force production. Nine subjects produced a downward tapping motion followed by vertical fingertip force against a rigid surface. We simultaneously recorded 3D fingertip force, plus the complete muscle coordination pattern using intramuscular electromyograms from all seven index finger muscles. We found that the muscle coordination pattern clearly switched from that for motion to that for isometric force ~65ms before contact (p=0.0004). Mathematical modeling and analysis revealed that the underlying neural control also switched between mutually incompatible strategies in a time-critical manner. Importantly, this abrupt switch in underlying neural control polluted fingertip force vector direction beyond what is explained by muscle activation-contraction dynamics and neuromuscular noise (p≤0.003). We further ruled out an impedance control strategy in a separate test showing no systematic change in initial force magnitude for catch trials where the tapping surface was surreptitiously lowered and raised (p=0.93). We conclude that the nervous system predictively switches between mutually incompatible neural control strategies to bridge the abrupt transition in mechanical constraints between motion and static force. Moreover because the nervous system cannot switch between control strategies instantaneously or exactly, there arise physical limits to the accuracy of force production upon contact. The need for such a neurally demanding and time-critical strategy for routine motion-to-force transitions with the fingertip may explain the existence of specialized neural circuits for the human hand.

Fine manipulation using fingertips is an integral part of the human identity. A fundamental element of manipulation is the acquisition of precision pinch: abruptly making contact with external surfaces to produce static force with the fingertips. Numerous studies show that the apparently trivial task of making contact using any limb is surprisingly difficult to understand or to successfully mimic with robots (e.g., (Lacquaniti and Maioli, 1987, 1989; Bizzi et al., 1992; Hogan, 1992; Wolpert et al., 1995; Gribble et al., 1998; Todorov, 2000; Ostry and Feldman, 2003; Kurtzer et al., 2005; Lackner and DiZio, 2005) and (Whitney, 1987; Kazerooni, 1990; Hogan, 1992; Hyde and Cutkosky, 1994; Akella and Cutkosky, 1995; Cavusoglu et al., 1997),

respectively). Contact discontinuously changes the mechanical constraints of the task. Therefore the joint torques (and muscle forces in turn) for producing motion and force with the end-point of a limb in a given direction are necessarily different (Hogan, 1985, 1992). However, the underlying neural control strategy need not change. One hypothesis known as impedance control in robotics and equilibrium point control in motor control proposes that to exert a limb force against a surface, we can simply regulate the viscoelastic muscle behavior so as to move the controlled "virtual" position of the limb inside the surface. In this case, a contact force emerges from the mismatch between actual and virtual position, without a direct need to code it in the neural signal (Feldman, 1986; Bizzi et al., 1992; Hogan, 1992; Hyde and Cutkosky, 1994; Mussa-Ivaldi and Bizzi, 2000; Ostry and Feldman, 2003). Alternatively, others hypothesize that the nervous system switches between two distinct control strategies, one to produce limb motion but that cannot produce limb force in the same direction as the motion, and vice versa. Hence, the contact transition is executed through accurate anticipation of contact time and careful feedforward/feedback control of joint torques (Whitney, 1976, 1987; Hogan, 1988; Kazerooni, 1990) or muscle activations (Lacquaniti and Maioli, 1987, 1989; Todorov, 2000). Regardless of where the reader may stand on this debate, to our knowledge contact transitions have not been studied in the realm of finger function.

Given the biomechanical (e.g., Valero-Cuevas et al., 2007) and neural (e.g., Penfield and Boldrey, 1937; Schieber and Hibbard, 1993; Scott, 2004) specialization of human fingers, it is unclear whether conclusions from studies of dynamic interactions of whole limbs with the environment extend to neuromuscular control of human fingers. Studies of typing (e.g., Kuo et al., 2006 and references therein) involve tasks where the contact surface is not rigid and the goal is not to produce a well-directed sustained static force against it. In contrast, the acquisition of precision pinch for manipulation of rigid objects requires abruptly making contact with the object to immediately generate well-directed static fingertip forces. Here we investigated whether the neural control of finger musculature switches when the index finger abruptly transitions from motion to isometric force production (i.e., a tap-to-push task). When we found that a switch occurred, we studied the timing, mechanical consequences and neuromuscular implications of the switch.

Methods

Consenting subjects (11m, 7f, age range 19-39 years, mean 22.8 years) with no history of neurological or hand pathology or injury participated in this study. This study was approved by Cornell University's Committee on Human Subjects. We recorded motions and forces in 18 subjects, and intramuscular electromyograms in 9 of them. Subjects wrapped the thumb and unused fingers of their dominant hand around a fixed horizontal dowel to produce force using their index finger against the flat, top surface of a cylindrical pedestal mounted on a 6-axis load cell (model 20E12A-I25, JR3 Inc., Woodland, CA). The surface position and height was adjusted such that the index finger was in a neutral ad-abduction posture and the metacarpo-phalangeal, proximal-interphalangeal and distal-interphalangeal joints in approximately 30, 45, and 15 degrees of flexion, respectively. Resembling our previous work (Valero-Cuevas, 2000), subjects wore a custom-molded thimble with a spherical Teflon bead embedded at its tip. This rigorously defined the mechanical task via a unique contact point and friction cone for force direction.

We instructed subjects to ramp-up fingertip force against a flat target surface to a self-selected high magnitude (~100% MVC) as quickly as possible (i.e., tap-to-push task). This ensured that the transition from motion to force production was indeed abrupt. They were instructed to, upon contact, keep the finger static and the force pointed vertically to the best of their ability. The trials started from three initial conditions—'relaxed', 'preactivated', and 'motion'. In the 'motion' condition, subjects tapped the target surface five times at a 1 Hz rhythm set by a metronome (1 s for the up-and-down motion) and pushed down on the surface at the end of the fifth cycle (Fig. 1a, blue traces show the last cycle). In the 'relaxed' condition, the subject rested the fingertip on the target surface for 2 metronome beats (i.e., 2 seconds) before pushing down (Fig. 1b, green traces). In the 'preactivated' condition, subjects produced a downward vertical force vector of a self-selected minimal magnitude for 2 metronome beats before pushing down (Fig. 1b, red traces). Subjects typically produced between 0.5 and 1 N of force magnitude in the 'preactivated' condition.

Electromyograms. The seven muscles actuating the index finger are flexor digitorum profundus, flexor digitorum superficialis, extensor indicis proprius, extensor digitorum communis, first lumbrical, first dorsal interosseous and first palmar interosseous. We recorded and digitally

processed EMG using fine-wire intramuscular electrodes from all seven muscles in 9 subjects using previously reported techniques (Valero-Cuevas, 2000). Amplified EMGs were sampled at 2000Hz, band-pass filtered 20Hz-800Hz, full-wave rectified, and normalized by the largest EMG level recorded during maximal voluntary contractions of that muscle. Maximal voluntary contractions of individual muscles were done immediately before and after fingertip force production, with the index finger braced in the same posture used during the study. We multiplied the normalized EMG from each muscle by its maximal muscle stress and then by its physiological cross sectional area values obtained by us in three prior biomechanical studies (Valero-Cuevas et al., 1998; Valero-Cuevas, 2000; Valero-Cuevas and Hentz, 2002) to find a time-varying muscle force vector (m(t)), the "muscle coordination pattern" (Valero-Cuevas et al., 1998; Valero-Cuevas, 2000, 2005)) [FP, FS, EI, EC, LUM, DI, PI]^T. Finally, we smoothed m(t)using a symmetric moving average with a 50ms window. As in our past work (Valero-Cuevas, 2000), the reference coordination pattern vector (m^{ref}) for each trial was defined as the average of m(t) during 100ms of peak force (always occurring >500ms after contact). We calculated the angle $(\theta(t))$ between $\underline{m}(t)$ at every sample and $\underline{m}^{\text{ref}}$ using the unit-vector dot-product formula given in equation 1:

$$\theta(t) = \cos^{-1} \left(\frac{\underline{m}(t) \circ \underline{m}^{\text{ref}}}{\|\underline{m}(t)\| \|\underline{m}^{\text{ref}}\|} \right)$$
(1)

where a larger θ means a larger misalignment of the measured coordination pattern with respect to the reference pattern and θ =0 means perfect alignment.

We found average of θ for each trial in six windows of 50ms width as shown in Fig. 2a and performed one-way repeated measures ANOVA to test whether θ differed across the six time-intervals. We applied a Tukey-Kramer adjustment for multiple comparisons when reporting p-values. We verified that the residuals were normally and identically distributed.

Fingertip force analysis. We used the vertical force (F_z) to detect contact or start of force-ramps. Force production was said to start when F_z exceeded 6 standard deviations above mean F_z during the relaxed, preactivated or no-contact period. Through trial-and-error, we found a threshold of 6 standard deviations to yield the most reliable detection of force onset and manually verified each

automatically detected force onset. We discarded trials where the finger slipped or bounced after contact, or if the flight phase during 'motion' trials was less than 400ms (despite the metronome).

We low-pass filtered (80Hz cut-off) the force data from all three axes before calculating the angular deviation of the force vector from vertical ($\phi_{\text{force}}(t)$). We then found $max(\phi_{\text{force}})$ and $var(\phi_{\text{force}})$ in the time-interval between +10ms and +65ms after contact (Fig. 3a-c). To be judiciously conservative, we excluded force data for the first 10ms after contact to remove high-frequency sensor noise transients that subdued typically by 5ms, and always well within 10ms (Fig. 1a). We also limited our analysis to +65ms because sensory feedback will affect force production subsequently (Venkadesan et al., 2007, and references therein). Both $max(\phi_{\text{force}})$ and $var(\phi_{\text{force}})$ were log-transformed to ensure normality. We then performed repeated measures ANOVA to test for differences in $max(\phi_{\text{force}})$ and $var(\phi_{\text{force}})$ between different initial conditions. We applied a Tukey-Kramer adjustment for multiple comparisons when reporting p-values.

Index finger model. To objectively evaluate the mechanical consequences of the contact transition on the initial angular deviation of the force vector, we developed a torque-driven planar index finger model with an ideal inelastic contact collision. This model produced motion when unconstrained, or force immediately upon contact with a surface (for non-slip conditions). Finger motion was modeled using a 3-link open kinematic chain; and initial force production as a four-bar linkage closed kinematic chain. We switched between the separate formulations for the motion and force production at contact.

We calculated net joint torques for motion ($\underline{\tau}_{\text{motion}}$) while ensuring that two features of our experimental trials were emulated. First, we designed model finger kinematics to emulate the subjects' preference to keep the distal phalanx vertical (i.e., perpendicular to the target surface). Second, to emulate the fact that subjects' fingertip made contact with a non-zero vertical velocity, we prescribed a sigmoidal vertical velocity profile for the model fingertip, starting with zero velocity 500ms before contact (highest finger posture) and peak velocity at contact. These two requirements uniquely specified the joint angles ($\underline{\varphi}(t)$) and joint angular velocities/accelerations throughout the motion phase. Given that the left hand side of equation

(2) is known for every instant of time during the motion phase, we directly calculated the unique joint torques for producing this motion.

$$M(\varphi)\ddot{\varphi} + C(\varphi,\dot{\varphi})\dot{\varphi} + \underline{N}(\varphi) = \underline{\tau}_{\text{motion}}$$
(2)

where $\underline{\varphi}$ is the vector of joint angles, M represents the inertial properties of the finger, C represents Coriolis and centrifugal forces on each phalanx, and N is the gravitational term.

The dynamical equation for initial force production when the fingertip makes contact with the surface is given by:

$$M(\underline{\varphi})\dot{\underline{\varphi}} + C(\underline{\varphi},\dot{\underline{\varphi}})\dot{\underline{\varphi}} + \underline{N}(\underline{\varphi}) + A(\underline{\varphi})^{T}\underline{f} = \underline{\tau}_{\text{force}}$$
where, $\underline{f} = (AM^{-1}A^{T})^{-1}(AM^{-1}(\underline{\tau}_{\text{force}} - C\dot{\underline{\varphi}} - \underline{N}) + \dot{A}\dot{\underline{\varphi}})$
(3)

where the posture dependent matrix A is the manipulator Jacobian that maps joint angular velocities to translational velocities of the fingertip and \underline{f} is the fingertip force vector produced when in contact with a surface. The beaded thimble used in the experiment precludes the fingertip from producing any torques while maintaining a static posture (see Valero-Cuevas et al., 1998) for a detailed description of the torque output of the fingertip). By definition, the unique joint torques needed to produce static vertical force ($\underline{\tau}_{\text{force}}$) are calculated by setting joint angular velocities and accelerations to zero in equation (3), i.e., $\underline{\tau}_{\text{force}} = A(\underline{\varphi})^{\text{T}} \underline{f} + \underline{N}(\underline{\varphi})$, where \underline{f} is the desired fingertip force vector.

We calculated $\underline{\tau}_{\text{motion}}(t)$, such that under the assumptions outlined for equation (2), it would take 500ms to travel from the height of the MCP joint to the height of the target. Also, the posture at contact emulated the reference posture used in our experiments, namely, 30, 45, and 15 degrees of flexion, from the proximal to the distal joints, respectively. We calculated joint torques at contact such that for the reference contact posture, $\underline{\tau}_{\text{force}}$ would produce static vertically oriented fingertip force vector of 0.15 N in magnitude. We simulated various durations (0ms to 65ms) of transition between $\underline{\tau}_{\text{motion}}$ and $\underline{\tau}_{\text{force}}$, as well as various errors in timing, i.e., the instant when the transition is completed (0ms to 20ms before contact occurs). We assumed an ideal inelastic collision (i.e., fingertip and joint motions come to a standstill upon contact). This allowed us to examine the mechanical consequences (i.e., causal relationships) between a non-

instantaneous transition in joint torques and initial misdirection in fingertip force vector upon contact—independently of the viscoelastic properties of the finger and collision dynamics.

Test of impedance control. We directly tested whether impedance control was used in a parallel study with six consenting subjects (3 m, 3f, avg. age 19.5 yrs, range 19-20 yrs.) in which EMG was not recorded. The task was identical to the with motion condition, with the difference that blindfolded subjects, while wearing the thimble, continuously tapped a 50 mm diameter rough sensor surface. Each tap motion lasted 3 seconds: the up-down tapping motion lasted 1 s as in the "motion" initial condition, followed by a 2 s period when subjects pushed to a self-selected low force (~ 25% MVC). Each subject performed a total of 150 taps in 10 batches of 15 taps. For all taps a robot lowered the surface to touch a bell, to allow the subject to phase-lock their tapping cadence, and then randomly raised the surface to either the reference height (in 95% of the taps) or to a different height (in 5% of the taps). The surface height for the 5% of "catch" trials was selected at random from a uniform distribution with ±6mm range. This prevented the blindfolded subject from using auditory cues to identify catch trials. The dependent variable for the regression (Fig. 5) was peak ||F|| for t=+10ms to t=+65ms after contact, normalized by the steady-state force the subjects reached at each tap. The variability in steady state force across subjects precluded our detecting systematic changes (if any) in initial force magnitude with surface height. Thus, we used normalization as a means to best detect a systematic change in initial force magnitude across trials with disparate self-selected steady-state static force magnitude.

Results

The 7D muscle coordination patterns ($\underline{m}(t)$) for motion (Fig. 2a, magenta boxes) and force production (Fig. 2a, blue boxes) were significantly different ($\Delta\theta \ge 20^{\circ}$, p<0.0001). However, even 65ms before contact (shaded box in Fig. 2a, during finger motion), the coordination pattern had already changed abruptly (in a span of ~60ms) and was significantly different from the preceding periods of finger motion (Fig. 2a, magenta box at [-150,-100] vs. shaded box at [-90,40], $\Delta\theta = 14^{\circ}$, p=0.0004), but statistically indistinguishable from the pattern for static force production (Fig. 2a, cyan box at [+20,+70] vs. shaded box at [-90,40], $\Delta\theta = 6^{\circ}$, p=0.28). This

clear and abrupt transition between coordination patterns occurred before contact could alter the mechanical condition, i.e., the switch in muscle coordination pattern cannot be explained by the onset of contact. Moreover, the coordination pattern ($\underline{m}(t)$) after contact was well aligned with $\underline{m}^{\text{ref}}$, the reference pattern for maximal static force production (cyan boxes in Fig. 2a, $\theta < 20^{\circ}$).

In addition, the increase in the vector magnitude of the muscle coordination pattern parallels that for the vector direction but is initiated later (i.e., closer to the contact time) (Fig. 2b). That is, the nervous system begins by increasing the alignment of the coordination pattern vector with that for force production over 100ms before contact (Fig. 2a). In contrast, the vector magnitude of the coordination pattern begins to increase to match that for initial force production less than 70ms before contact (Fig. 2b). Thus we find that the transformation of the muscle coordination pattern vector from that for motion to that for static force resembles a nonlinear interpolation.

A mathematical analysis of the time course of the transition of muscle coordination patterns shows that there was necessarily a switch between mutually incompatible underlying neural control strategies: from one for finger motion to another for fingertip force production (See Supporting Online Material for full details). By "incompatible" neural control strategies we mean incompatible with each other by virtue of each strategy being able to meet only one set of mechanical constraints: either those for motion or those for force. Briefly, our analysis formalizes the following statement: given that the finger's mechanical state and external constraints do not change as it approaches contact, a change in muscle coordination pattern necessitates a change in the underlying neural control strategy. That is, the switch in muscle coordination pattern is of neural origin because it cannot be explained by the mechanical transition at contact. The proof of this argument follows the reductio ad absurdum argument. If one assumes the underlying neural control strategy to be constant as the finger undergoes contact, then the resulting relationship among muscle coordination patterns directly contradicts our experimental finding that they change rapidly before contact. This result applies even when the underlying neural control strategy undergoes changes compatible with neural and muscle redundancy (e.g., changes in neural signals that do not affect the muscle coordination patterns). Importantly, this analytical conclusion holds for a general underlying neural control strategy that could, for example, encode either muscle forces directly, or other properties of the neuromuscular system like motoneuron excitability.

We also found that the abrupt switch in underlying neural control strategy polluted fingertip force vector direction beyond what is explained by muscle activation-contraction dynamics (Zajac, 1989), neuromuscular noise (Harris and Wolpert, 1998), and premotor planning (Sober and Sabes, 2005). We used two quantifiers of fluctuations in force production between +10 and + 65ms after contact (Fig. 3)—peak angular deviation ($\phi_{force}(t)$) of the fingertip force vector from the vertical ($max(\phi_{force})$) and its variance ($var(\phi_{force})$). Repeated measured analysis of variance found both $max(\phi_{force})$ and $var(\phi_{force})$ to be significantly larger for the 'motion' initial condition, and significantly and progressively lower for the 'relaxed' and 'preactivated' initial conditions (Fig. 3; highest posthoc pairwise p value <0.018).

Importantly, our mechanical torque-driven planar index finger model found that switching between control strategies is time-critical, and the likely source of pollution in force direction. Such force misdirection upon contact is predicted to occur in this model even though the contact collision is ideally inelastic and the viscoelastic properties of the finger and force transducer are not present. If the switch in neural control strategy could occur instantaneously and exactly upon contact, i.e., resembling an ideal step function at contact, the model predicted the fingertip force vector to be perfectly perpendicular to the surface immediately after contact (origin in Fig. 4). However, a more realistic sample simulation compatible with muscle excitation-contraction delays where the transition takes 35ms to be completed and ends exactly at contact shows that the fingertip force misdirection at the instant of contact is at least 7° (Fig. 4), which is realistically compatible with our experimental results. Moreover, repeated iterations of the model show that the force vector misdirection is very sensitive to both the timing and duration of the transition. Force misdirection errors arise simply because transition duration and/or imprecise timing cause the finger to make contact in a posture different from the planned posture. Figure 4 underscores the time-criticality of this switching in control strategies because even small (i.e., 10ms) increases in both the onset and duration of the transition can lead to >60% increase of errors in initial force vector direction (e.g., vertical line at 35ms in Fig. 4). The effectiveness of compensatory strategies in the face of such time-criticality is addressed in the Discussion.

Lastly, a necessary prediction of impedance control is that force output ($\|\underline{F}\|$ shortly after contact) will systematically change with surface height. However, we saw no such systematic change in the catch trials where subjects tapped on the surreptitiously elevated/lowered surface (n=6, p=0.93, Fig. 5).

Discussion

By recording EMG from all muscles of the index finger, we found that muscle coordination patterns changed abruptly in a nonlinear, time-critical manner between characteristic 'motion' and 'force' patterns. Because this clear and abrupt transition occurred before contact could alter the finger's mechanical condition, our mathematical analysis finds this necessarily reflects a switch between mutually incompatible underlying neural control strategies. Additionally, because force output did not vary systematically with surreptitious changes in the tapping surface height, we could directly rule out impedance control as the dominant form of control. Importantly, we find that this switch between underlying neural control strategies results in pollution of the initial fingertip force vector direction above and beyond neuromuscular noise or muscle activation-contraction dynamics. A mechanical index finger model found that these unavoidable errors in initial force direction are a consequence of the inability of the nervous system to switch instantaneously and exactly between incompatible control strategies. Thus the physiological limitations of the neuromuscular system plus the time-criticality of this switching in control strategies conspire to impose physical limits on the accuracy of force production upon contact. We speculate that such a neurally demanding and time-critical strategy for the transition from the control of fingertip motion to force production may explain the existence of specialized neural circuits for the human hand.

Finding a switch between mutually incompatible underlying neural control strategies has important consequences to the study of motor control of the fingers. For human fingers, our findings challenge hypotheses like equilibrium point control that propose constant control strategies capable of bridging abrupt changes in mechanical constraints (Feldman, 1986; Bizzi et al., 1992; Gribble et al., 1998; Mussa-Ivaldi and Bizzi, 2000; Ostry and Feldman, 2003). A proposed advantage of equilibrium point control is that it can mediate transitions between

posture and movement "automatically," without the nervous system explicitly computing or actively controlling it (Ostry and Feldman, 2003). In contrast, our data and analysis show a clear example of the nervous system utilizing a neurally demanding and time-critical switch between mutually incompatible underlying neural control strategies to transition from motion to force production. Independently of current debates on plausible control strategies, our results support the more fundamental idea that the neural control of the fingers fits well within the emerging framework of hybrid control systems characterized by dynamical systems subject to continuous controls and discrete transitions (Guckenheimer, 1995; Branicky et al., 1998).

Our results reveal that the time-critical transformation of the muscle coordination pattern vector prior to contact resembles a nonlinear transformation. We find that the change in the vector direction of the muscle coordination pattern is well underway at least 100ms before contact (Fig. 2a). In contrast, the vector magnitude begins to change only within 70ms of contact (Fig. 2b). A linear transformation would cause simultaneous and proportional scaling of both the vector magnitude and direction. Three possible explanations come to mind (i) there exist neuromusculo-skeletal constraints which prevent or bias against the implementation of a linear transformation (e.g., neural coupling, motoneuron pool spillover, anatomical coupling among finger musculature); (ii) the limitations of EMG artifactually distort estimates of linearity of the transformation; or (iii) a nonlinear path is conducive to reducing errors in the fingertip trajectory, the finger posture at contact, and hence initial force production. We have previously presented fine-wire EMG evidence that the nervous system is able to control index finger muscles independently in a similar force production paradigm (Valero-Cuevas et al., 1998; Valero-Cuevas, 2000). This argues against neuro-musculo-skeletal constraints or EMG artifacts being the dominant explanation for the nonlinear transformation in our present data. By this process of elimination we speculate that, while the finger is still in motion, the nervous system reduces the deviation from the planned posture for contact by postponing the necessary increase in coordination pattern magnitude. Establishing whether this specific nonlinear transformation is task-optimal requires additional experimental and modeling work that is beyond the scope of this first report of the phenomenon. The time-criticality of this transformation is discussed below.

Our work extends current understanding of the control of finger musculature by showing that during abrupt transitions between neural control strategies, muscle physiology imposes physical limits to the accuracy of static force production upon contact. Our simulations quantify the mechanical sensitivity of initial force direction to the duration and timing of the switch between mutually incompatible strategies (Fig. 4). That is, switching between mutually incompatible control strategies for motion and static force will unavoidably pollute force production after contact if not done exactly and instantaneously. For realistic switching durations constrained at a minimum by 35ms of muscle activation-contraction dynamics (Zajac, 1989), deviations from a planned completion of the switching by even 10ms increase force misdirection by >60% (Fig. 4, vertical line at 35ms in duration). In the biological system, timing errors of ~10ms are tenable given unavoidable neuromuscular noise (Harris and Wolpert, 1998) and physiological delays (Venkadesan et al., 2007, and references therein). It is conceivable that the nervous system could plan joint torques for motion using compensatory strategies so that the finger lands in the planned contact posture. However, any such anticipatory motor planning does not, in practice, suffice to cancel out errors in initial force direction because it necessarily involves at the very least an accurate estimate of the time of contact with the surface. As mentioned above, even a 10ms uncertainty in the estimate of contact time suffices to incur substantial errors in initial force direction of the magnitudes we saw experimentally. This may explain why our healthy and motivated subjects always exhibited a misdirected initial force. After this initial misdirection, musculoskeletal viscoelastic properties and sensory feedback control will undoubtedly take effect in the real finger and cause the observed force oscillations and subsequent refinement of force direction (Fig. 3).

Our experimental design allowed the disambiguation between mechanical, muscular and neural sources of inaccuracies of force production. Comparing across the 'motion', 'preactivated' and 'relaxed' initial conditions allowed us to directly identify fluctuations in force direction for the first 65ms after onset as arising from switching between neural control strategies, as distinct from the effects of premotor planning and muscle activation-contraction dynamics. As previously shown by Valero-Cuevas (2000), the 'preactivated' condition likely only requires scaling of the coordination pattern and is therefore only affected by neuromuscular noise. The 'relaxed' condition, on the other hand, is additionally affected by the selection and

implementation of the motor program (e.g., premotor planning plus muscle activation-contraction dynamics).

We now discuss the relationships of our findings to past work on anticipatory motor control, and the limitations of our approach. Multiple studies have characterized anticipatory control in the limbs of humans and animals, (i) for smooth motion-force tasks for limbs subject to contacting (e.g., manipulanda experiments: Shadmehr and Mussa Ivaldi, 1994; Lackner and DiZio, 2005) and non-contacting (e.g., Coriolis force experiments: Lackner and DiZio, 2005, and references therein) force fields, (ii) during abrupt postural perturbations associated with catching (Lacquaniti and Maioli, 1989; Lacquaniti et al., 1992), and (iii) and animal studies of posture vs. ground-reaction force control (Lacquaniti and Maioli, 1994) or posture vs. movement control (Kurtzer et al., 2005). Our results agree with their findings and conclusions to the extent that the nervous system can and does effectively anticipate changes in task constraints. In addition, the timing of the onset of anticipatory changes in EMG of ~100ms are similar to those found previously (Lacquaniti and Maioli, 1989). However, anticipatory control in our task is different from braking to mitigate a collision or from stiffening before catching. We did not observe any anticipatory braking because the goal of our task required a collision so as to be able to ramp up force production as rapidly as possible, as evinced by the spikes in vertical force at contact (Fig. 1a). To our knowledge, this is the first study to record complete muscle coordination patterns and full 3D force vectors while fingertips abruptly contact a surface to produce static force. This enabled us to use careful mathematical analysis and mechanical simulations to (i) uncover the nonlinear nature of the anticipatory transformation of muscle coordination patterns; (ii) detect the switch in the underlying neural control strategy; and (iii) characterize the consequences of this switch to the accuracy of initial force production. Unlike previous reports, our conclusions are independent of any one specific theory of motor control (e.g., equilibrium point hypothesis, direct cortical control of muscles, etc). We believe the limitations of our approach do not challenge the validity of our conclusions. Although the use of a custom-molded thimble may appear unnatural, its potential drawbacks are outweighed by the benefits of a well-defined contact condition (e.g., fingernail length and shape, skin dryness). This has allowed us to obtain high-fidelity biomechanical recordings that can be well approximated by a model (Valero-Cuevas et al., 1998; Valero-Cuevas, 2000). In addition, the use of the thimble does approximate

precision pinch acquisition of small, irregularly shaped or slippery objects. Other considerations point us to future studies such as the effect of lengthy practice on the neural strategy, or the inclusion of specialized populations such as microsurgeons or pianists. Similarly, the torquedriven model of the index finger can be further explored though parameter sensitivity analysis (e.g., Santos and Valero-Cuevas, 2006) or extended to include musculature, sophisticated control strategies, and contact collision models.

In conclusion, contacting a surface with the fingertip to produce static force requires: (i) accurate prediction of when contact would occur and (ii) time-critical switching between underlying neural control strategies. For these reasons, dedicated neural circuits are likely used for representation of motion and force similar to the observation for control of the arm in monkeys (Kurtzer et al., 2005). Interestingly, it is known that in humans direct corticospinal projections to the hand muscles are more prevalent than for the limbs (Scott, 2004). Therefore our results could provide a functional insight into an important evolutionary feature of the human brain: the disproportionately large sensory and motor representations of the hand (Penfield and Boldrey, 1937). If indeed the nervous system faced evolutionary pressures to precisely and anticipatorily control even routine tasks like rapid acquisition of precision pinch, the sensorimotor cortical representations of our fingers would naturally reflect those requirements for careful timing of motor actions and fine independent control of the finger muscles. Finally, our finding of the stringent sensorimotor demands of finger contact transitions might also help understand why precision pinch and finger tapping are skills that take years to develop in young children (Forssberg et al., 1991) and are so vulnerable to neurological degeneration and aging (Cole et al., 1998).

References

- **Akella PN, Cutkosky MR** (1995) Contact transition control with semiactive soft fingertips. IEEE Transactions on Robotics and Automation 11:859-867.
- **Bizzi E, Hogan N, Mussaivaldi FA, Giszter S** (1992) Does the Nervous-System Use Equilibrium-Point Control to Guide Single and Multiple Joint Movements. Behavioral and Brain Sciences 15:603-613.
- **Branicky MS, Borkar VS, Mitter SK** (1998) A unified framework for hybrid control: Model and optimal control theory. IEEE Transactions on Automatic Control 43:31-45.
- **Cavusoglu M, Yan J, Sastry S** (1997) A hybrid system approach to contact stability and force control in robotic manipulators. Intelligent Control, 1997 Proceedings of the 1997 IEEE International Symposium on:143-148.
- Cole KJ, Rotella DL, Harper JG (1998) Tactile impairments cannot explain the effect of age on a grasp and lift task. Experimental Brain Research 121:263-269.
- **Feldman A** (1986) Once more on the equilibrium-point hypothesis (lambda model) for motor control. J Mot Behav 18:17-54.
- **Forssberg H, Eliasson A, Kinoshita H, Johansson R, Westling G** (1991) Development of human precision grip I: Basic coordination of force. Experimental Brain Research 85:451-457.
- **Gribble PL, Ostry DJ, Sanguineti V, Laboissiere R** (1998) Are complex control signals required for human arm movement? Journal of Neurophysiology 79:1409-1424.
- **Guckenheimer J** (1995) A Robust Hybrid Stabilization Strategy for Equilibria. IEEE Transactions on Automatic Control 40:321.
- **Harris CM, Wolpert DM** (1998) Signal-dependent noise determines motor planning. Nature 394:780-784.
- **Hogan N** (1985) The Mechanics of Multi-Joint Posture and Movement Control. Biological Cybernetics 52:315-331.
- **Hogan N** (1988) On the Stability of Manipulators Performing Contact Tasks. IEEE Journal of Robotics and Automation 4:677-686.
- **Hogan N** (1992) Control of contact in robots and biological systems. IEEE Engineering in Medicine and Biology Magazine 11:81-82.
- **Hyde J, Cutkosky M** (1994) Controlling contact transition. Control Systems Magazine, IEEE 14:25-30.

- **Kazerooni H** (1990) Contact instability of the direct drive robot when constrained by a rigid environment. Automatic Control, IEEE Transactions on 35:710-714.
- **Kuo PL, Lee DL, Jindrich DL, Dennerlein JT** (2006) Finger joint coordination during tapping. J Biomech 39:2934-2942.
- **Kurtzer I, Herter TM, Scott SH** (2005) Random change in cortical load representation suggests distinct control of posture and movement. Nature Neuroscience 8:498-504.
- **Lackner JR, DiZio P** (2005) Motor control and learning in altered dynamic environments. Current Opinion in Neurobiology 15:653-659.
- **Lacquaniti F, Maioli C** (1987) Anticipatory and reflex coactivation of antagonist muscles in catching. Brain Res 406:373-378.
- **Lacquaniti F, Maioli C** (1989) The role of preparation in tuning anticipatory and reflex responses during catching. J Neurosci 9:134-148.
- **Lacquaniti F, Maioli C** (1994) Independent control of limb position and contact forces in cat posture. J Neurophysiol 72:1476-1495.
- **Lacquaniti F, Borghese NA, Carrozzo M** (1992) Internal models of limb geometry in the control of hand compliance. J Neurosci 12:1750-1762.
- **Mussa-Ivaldi FA, Bizzi E** (2000) Motor learning through the combination of primitives. Philosophical Transactions of the Royal Society of London Series B-Biological Sciences 355:1755-1769.
- **Ostry D, Feldman A** (2003) A critical evaluation of the force control hypothesis in motor control. Experimental Brain Research 153:275-288.
- **Penfield W, Boldrey E** (1937) Somatic motor and sensory representation in the cerebral cortex of man as studied by electrical stimulation. Brain 60:389-443.
- **Santos VJ, Valero-Cuevas FJ** (2006) Reported anatomical variability naturally leads to multimodal distributions of Denavit-Hartenberg parameters for the human thumb. IEEE Trans Biomed Eng 53:155-163.
- **Schieber MH, Hibbard LS** (1993) How somatotopic is the motor cortex hand area? Science 261:489-492.
- **Scott SH** (2004) Optimal feedback control and the neural basis of volitional motor control. Nature Reviews Neuroscience 5:534-546.
- **Shadmehr R, Mussa Ivaldi FA** (1994) Adaptive Representation of Dynamics During Learning of a Motor Task. Journal of Neuroscience 14:3208-3224.

- **Sober SJ, Sabes PN** (2005) Flexible strategies for sensory integration during motor planning. Nat Neurosci 8:490-497.
- **Todorov E** (2000) Direct cortical control of muscle activation in voluntary arm movements: a model. Nature Neuroscience 3:391-398.
- **Valero-Cuevas FJ** (2000) Predictive modulation of muscle coordination pattern magnitude scales fingertip force magnitude over the voluntary range. J Neurophysiol 83:1469-1479.
- **Valero-Cuevas FJ** (2005) An integrative approach to the biomechanical function and neuromuscular control of the fingers. J Biomech 38:673-684.
- **Valero-Cuevas FJ, Hentz VR** (2002) Releasing the A3 pulley and leaving flexor superficialis intact increases pinch force following the Zancolli lasso procedures to prevent claw deformity in the intrinsic palsied finger. J Orthop Res 20:902-909.
- **Valero-Cuevas FJ, Zajac FE, Burgar CG** (1998) Large index-fingertip forces are produced by subject-independent patterns of muscle excitation. J Biomech 31:693-703.
- Valero-Cuevas FJ, Yi JW, Brown D, McNamara III RV, Paul C, Lipson H (2007) The tendon network of the fingers performs anatomical computation at a macroscopic scale. IEEE Trans Biomed Eng 54:1161-1166.
- **Venkadesan M, Guckenheimer J, Valero-Cuevas FJ** (2007) Manipulating the edge of instability. J Biomech 40:1653-1661.
- Whitney D (1976) Force feedback control of manipulator fine motions. Productivity:687-693.
- **Whitney D** (1987) Historical Perspective and State of the Art in Robot Force Control. The International Journal of Robotics Research 6:3.
- Wolpert DM, Ghahramani Z, Jordan MI (1995) An Internal Model for Sensorimotor Integration. Science 269:1880-1882.
- **Zajac FE** (1989) Muscle and tendon: properties, models, scaling, and application to biomechanics and motor control. Crit Rev Biomed Eng 17:359-411.

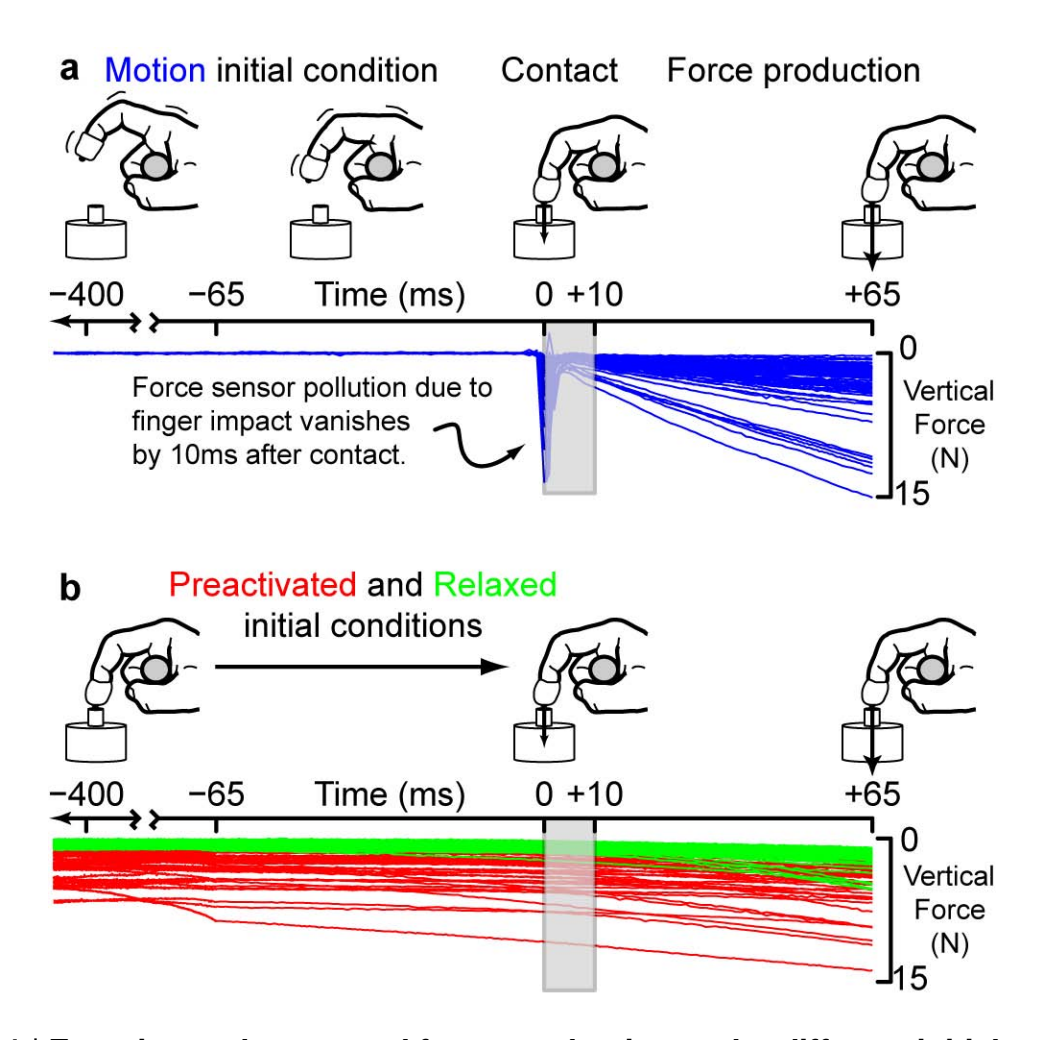


Figure 1 | **Experimental setup and force production under different initial conditions. a**, For the 'motion' initial condition, subjects tapped the surface 5 times before pushing against it to maximize vertical force. The blue traces show vertical force data from all subjects. Data from the first 10ms (grey box) were excluded to remove high-frequency impact sensor noise transients that subdued typically by 5ms, and always well within 10ms. **b**, For the 'relaxed' (green) and 'preactivated' (red) initial conditions, subjects produced force-ramps in a static posture (no prior finger motion), and from nearly zero, or low force (~25% of maximal voluntary force), respectively.

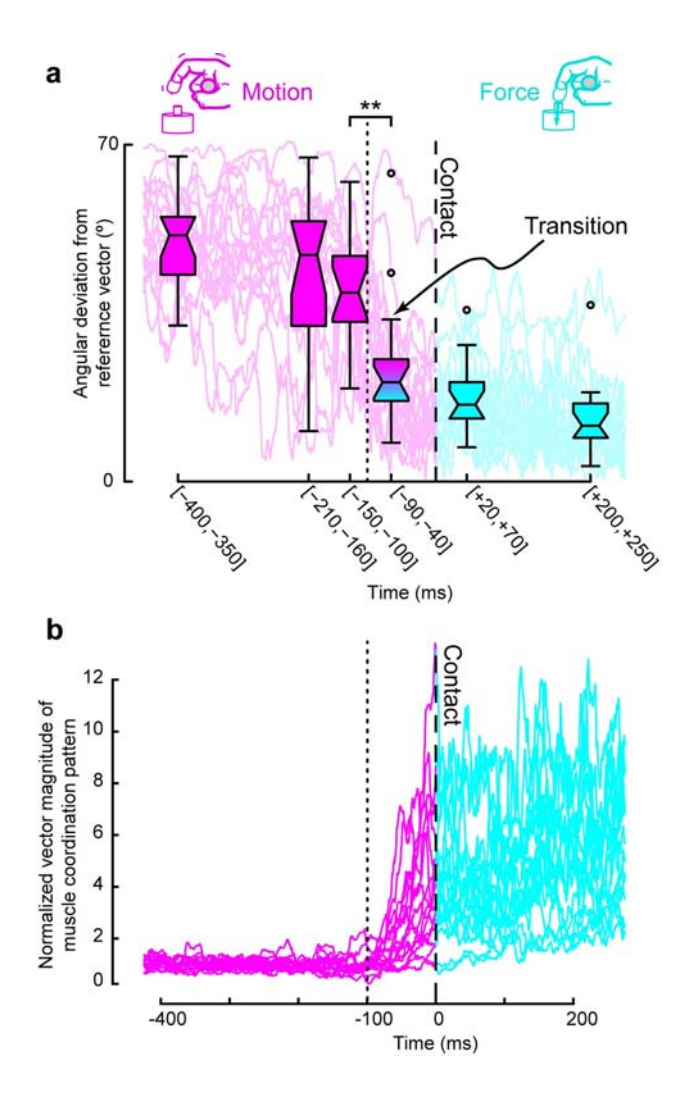


Figure 2 | Switch in direction and magnitude of the muscle coordination pattern vector between motion and static force production. a, Muscle coordination patterns (magenta and cyan traces) are represented by their angular deviation (θ) from a reference coordination pattern (namely, the coordination pattern when fingertip force was the highest). The box plots are 50ms wide averages of θ . The central line is the median, the notches are the robust 95% confidence limits of the median, the lower and upper limits of the box are the quartile limits, whiskers lengths are 1.5 times the interquartile distance and outliers are shown with circular markers. The switch between patently different patterns for motion and force occurred very abruptly and before contact (the shaded box extending from -90ms to -40ms). b, The vector magnitude of the muscle coordination pattern was normalized by the mean magnitude for each trial during the first 200ms of motion. This enabled an objective comparison of how the magnitude scaled over the time-course of each trial. The vector magnitude was higher even for initial force production compared to the motion phase. Much like the switch in vector direction (Fig. 2a), this increase in vector magnitude started before contact. However, unlike the vector direction that started switching over 100ms before contact, the vector magnitude started increasing less ~70ms before contact.

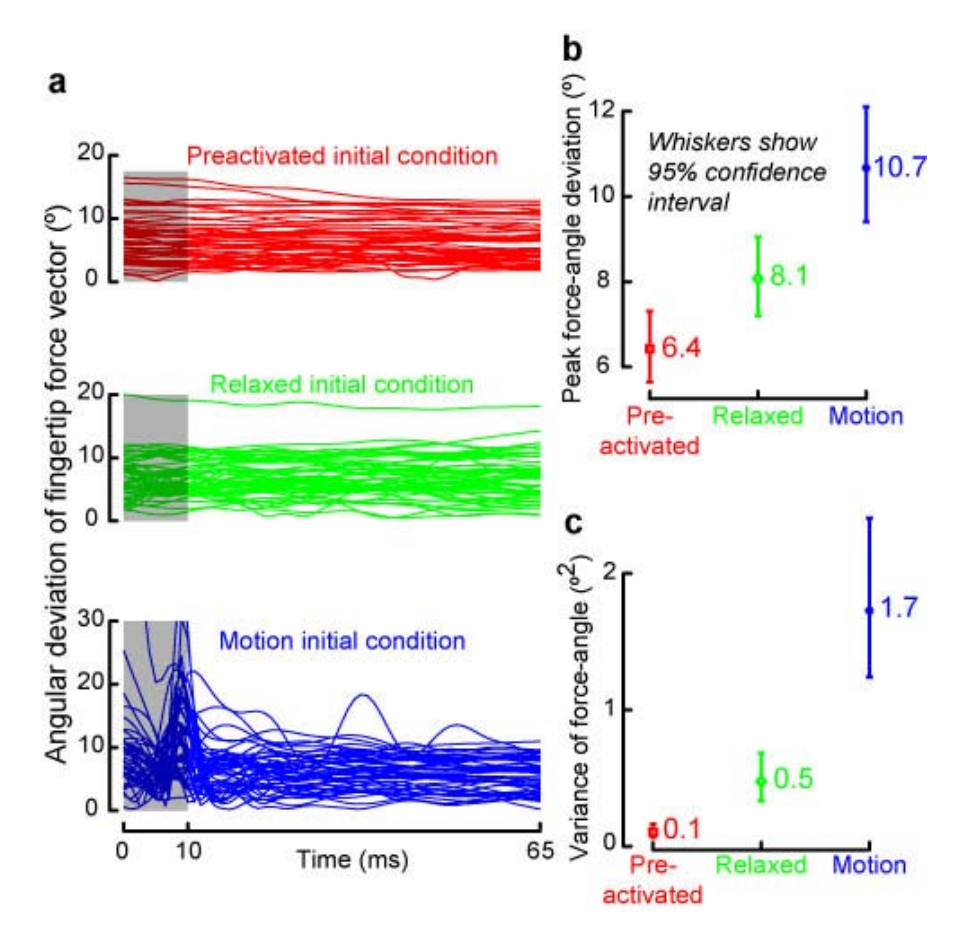


Figure 3 | Fluctuations in direction of the fingertip force vector after finger contact. a, Force angle data ($\phi_{force}(t)$) from all subjects for all three initial conditions. The first 10ms are greyed out and excluded for all analyses. Even for the remaining time-segment, the force direction appears to fluctuate much more for the motion condition than for either the relaxed (green) or preactivated (red) conditions. The peak force angle deviation for the 'motion' condition (blue) occurs around 8ms. We are conservative in our analyses by excluding the first 10ms because the force data were clearly reliable well before 8ms (blue traces in Fig. 1a). b, The peak force angle deviation ($max(\phi_{force})$) decreased from motion to relaxed to preactivated conditions. All differences were statistically significant. c, The variance in force direction ($var(\phi_{force})$) also decreased from motion to relaxed to preactivated conditions and all differences were statistically significant.

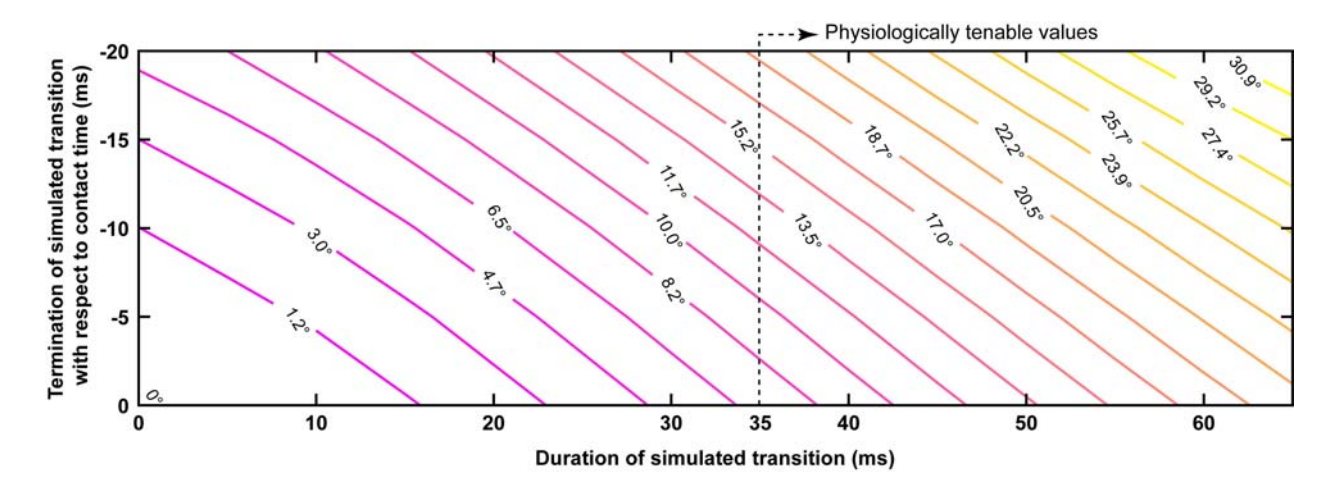


Figure 4 | Simulations reveal that just muscle activation-contraction dynamics impose a physical limit on directional accuracy of the initial fingertip force vector upon contact. The labeled contour lines show the misdirection of the initial fingertip force vector with respect to the surface normal. The abscissa shows the duration of the transition between the joint torque pattern for motion and that for force; and the ordinate shows inaccuracies in the timing of this transition, represented by its termination time with respect to contact time. For physiologically tenable values of transition duration (> 35ms), the initial fingertip force vector is misdirected by at least 7°, and the misdirection increases by over 60% for every 10ms increase in timing inaccuracy (contour values along vertical dotted line at 35ms abscissa).

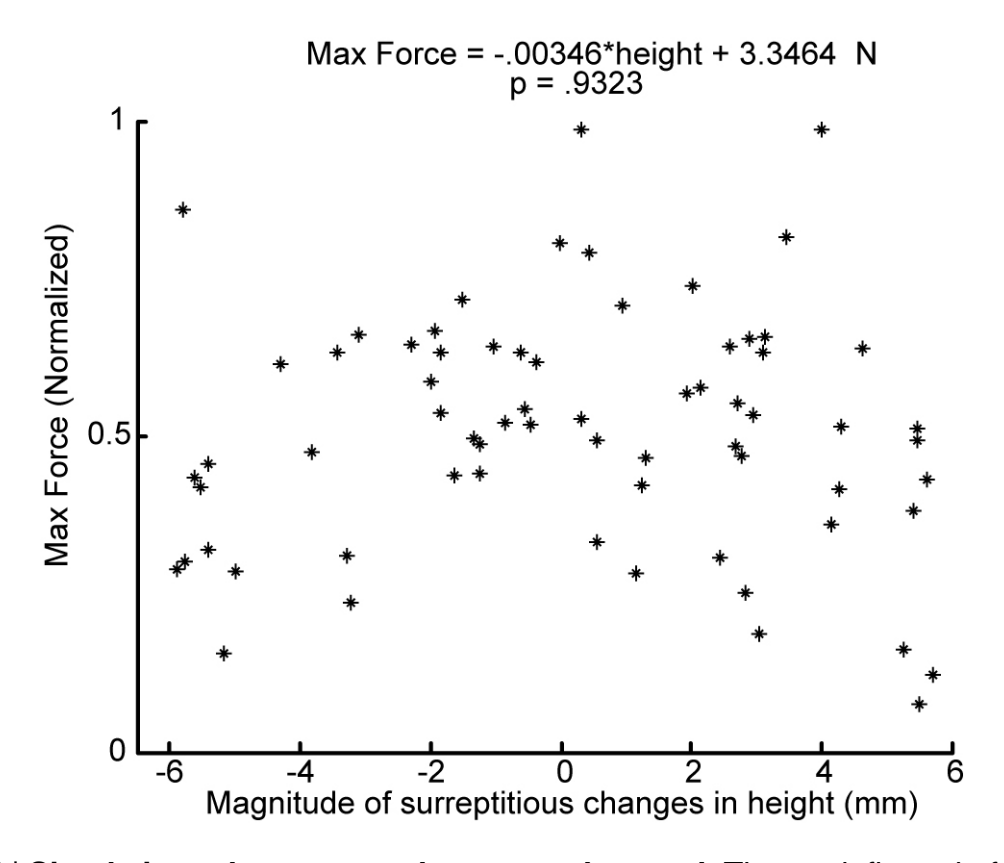


Figure 5 | **Simple impedance control was not observed.** The peak fingertip force magnitude (ordinate) within 65ms after contact (the first 10ms excluded) did not change systematically with surreptitious changes in the surface height (abscissa). This shows that a simple impedance control strategy could not have been the dominant form of control for finger contact transitions.

Supporting Online Material for

Neural control of motion-to-force transitions with the fingertip

Madhusudhan Venkadesan ^{a,d} and Francisco J. Valero-Cuevas ^{b,c,d,*}

^aDepartment of Mathematics, Cornell University, Ithaca, NY, USA

^bDepartment of Biomedical Engineering, University of Southern California, Los Angeles, CA, USA

^cDivision of Biokinesiology & Physical Therapy, University of Southern California, Los Angeles, CA, USA

^dSibley School of Mechanical & Aerospace Engineering, Cornell University, Ithaca, NY, USA

Contents

- S1 Notation
- S2 Joint torques for producing motion and static force are mutually incompatible
- S3 Neuromuscular model of the index finger
 - S3.a Muscle forces and their relation to joint torques
 - S3.b Muscle forces arise from neural control signals and mechanics
 - S3.c Affine approximation
- S4 Proof of switching between mutually incompatible underlying neural control strategies
 - S4.a Validation of simplified affine model
 - S4.b Proof by reductio ad absurdum
- S5 Generalizing to include neural and muscle redundancy
 - S5.a Generalization by considering neural redundancy
 - S5.b Consideration of muscle redundancy

List of Figures

- S1 Schematic for a model of index finger tapping.
- S2 Schematic of the main experimental finding.
- S3 Summary of variables used in proof.

* To whom correspondence should be addressed. *Email addresses: mv72@cornell.edu (Madhusudhan Venkadesan), fv24@cornell.edu (Francisco J. Valero-Cuevas).

S1 Notation

Throughout this supplementary text, underlined variables are vectors and "hatted" variables are unit vectors. For example, \underline{a} is a vector and \hat{a} is its corresponding unit vector, i.e., $\hat{a} = \underline{a}/\|\underline{a}\|$. We use lower case, *italicized* letters for scalars and **boldface** for functions and operators.

S2 Joint torques for producing motion and static force are mutually incompatible

We saw from the main text (equations 1 and 2) how the production of free finger motion and well-directed static force production when in contact with a surface are produced by very different equations. As a consequence, at a given posture, the joint torque patterns for producing motion and static force are different from each other. Not only that, the two joint torque patterns are mutually incompatible, i.e., the torque pattern for producing motion in a specific direction cannot produce well-directed static force in the same direction and *vice versa*. Our experimental observation of starkly different muscle coordination patterns for motion and force is not surprising given that mechanics necessarily dictates different joint torques for motion and force.

S3 Neuromuscular model of the index finger

A dynamical model of the index finger is depicted in Fig. S1. It is necessary for our purposes to separate the various components—neural signals $(\underline{u}(t))$, muscle forces $(\underline{m}(t))$, joint torques $(\underline{\tau}(t))$, finger mechanical condition $(\underline{x}(t))$, a vector of joint angles $\underline{\varphi}$, angular velocities $\underline{\dot{\varphi}}$ and external forces \underline{f}), and external boundary conditions (contact or no-contact). We use a generic model, where the various transformations (e.g., $\underline{\mathbf{g}}$ that generates muscle forces) could be as simple as linear functions or as complex as nonlinear differential equations. A simple torque-driven model was used in the main text (equations 1 and 2). Muscle models could be of various complexities. For example, a simple model of muscle could produce muscle

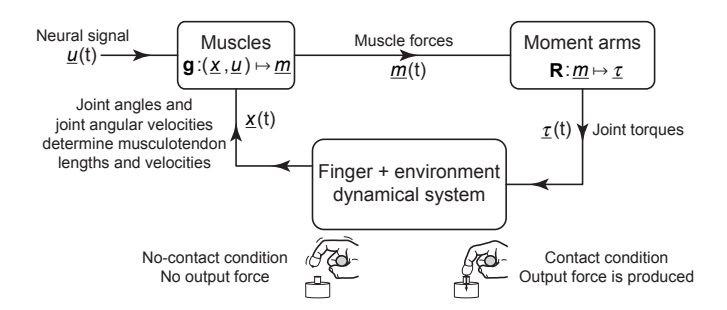


Fig. S1. Schematic for a dynamical model of index finger tapping. The model as shown is fairly generic. Each module $(\underline{\mathbf{g}}, \mathbf{R})$, finger + environment dynamics) is in general a nonlinear dynamical system.

force linearly proportional to the neural signal, but nonlinearly dependent on musculotendon length and velocity (force-length and force-velocity properties of muscle (Zajac, 1989)). In contrast, if the neural signal did not encode muscle forces directly, but something like muscle equilibrium length or neural thresholds (Feldman, 1986, Gribble et al., 1998, Ostry and Feldman, 2003), the function $\underline{\mathbf{g}}$ will be a relatively complicated and nonlinear function of both the neural signal as well as the musculotendon lengths and velocities.

Redundancy is built-in to typical models at both neural and muscular levels because $\dim(\underline{u}(t)) > \dim(\underline{m}(t)) > \dim(\underline{\tau}(t))$. A redundant neural system will allow for a null-space within which "preparatory" or "anticipatory" changes in the neural control signals can happen. For example, changes in the neural control signals would not manifest themselves as changes in muscle forces. Similarly, redundant musculature will allow for changes in muscle forces that will not lead to changes in the net joint torque.

S3.a Muscle forces and their relation to joint torques

Muscle forces are translated into joint torques by the musculotendon moment arms for each muscle about each joint. In general, it could be some nonlinear function of posture.

$$\underline{\tau}(t) = \mathbf{R}\underline{m}(t) \tag{S3.1}$$

where, R is the moment arm matrix.

S3.b Muscle forces arise from neural control signals and mechanics

Muscle forces are not solely a consequence of either the neural signal or the mechanical condition of the finger (\underline{x} , i.e., $\varphi, \dot{\varphi}, f$). Rather, it is a function of both. Mathematically stated,

$$\underline{m}(t) = \mathbf{g}(\underline{x}(t), \underline{u}(t)) \tag{S3.2}$$

where, g is a nonlinear function that can accommodate various types of controllers including direct control of muscle forces or joint torques (e.g., Todorov, 2000), motoneuronal threshold control (e.g., Ostry and Feldman, 2003), etc.

S3.c Affine approximation

We now simplify equation (S3.2) to a linear model. The Taylor series expansion for the function $\underline{\mathbf{g}}$ about some nominal point $(\underline{x}_0, \underline{u}_0)$ is,

$$\underline{\mathbf{g}}(\underline{x},\underline{u}) \approx \underline{\mathbf{g}}(\underline{x}_0,\underline{u}_0) + \frac{\partial \underline{\mathbf{g}}}{\partial \underline{x}} \bigg|_{(\underline{x}_0,\underline{u}_0)} (\underline{x} - \underline{x}_0) + \frac{\partial \underline{\mathbf{g}}}{\partial \underline{u}} \bigg|_{(\underline{x}_0,\underline{u}_0)} (\underline{u} - \underline{u}_0)$$
(S3.3a)

Let us consider first the special case where $\underline{x} = \underline{x}_0$. Then, the Taylor series approximation can be further simplified to,

$$\mathbf{g}(\underline{x}, \underline{u}) \approx \Psi \underline{u} + (\mathbf{g}(\underline{x}_0, \underline{u}_0) - \Psi \underline{u}_0)$$
 (S3.3b)

where,

$$\Psi = \frac{\partial \mathbf{g}}{\partial \underline{u}} \bigg|_{(\underline{x}_0, \underline{u}_0)}$$
 (S3.3c)

Without loss of generality, we can set the constant term (not dependent on \underline{u}) to 0 in equation (S3.3b). Therefore, we are now left with the following simplified model that, at \underline{x}_0 , maps the neural control signal to muscle forces when the control signal is close to some nominal signal \underline{u}_0 .

$$m = \Psi(x_0)u \tag{S3.4}$$

To emphasize the dependence on mechanical condition, we only show the dependence of Ψ on \underline{x}_0 , although it clearly also depends on \underline{u}_0 .

S4 Proof of switching between mutually incompatible underlying neural control strategies

We show in Fig. S2 an abstraction of the main experimental finding of a switch in muscle coordination pattern before contact occurs. The finger's mechanical condition is nearly identi-

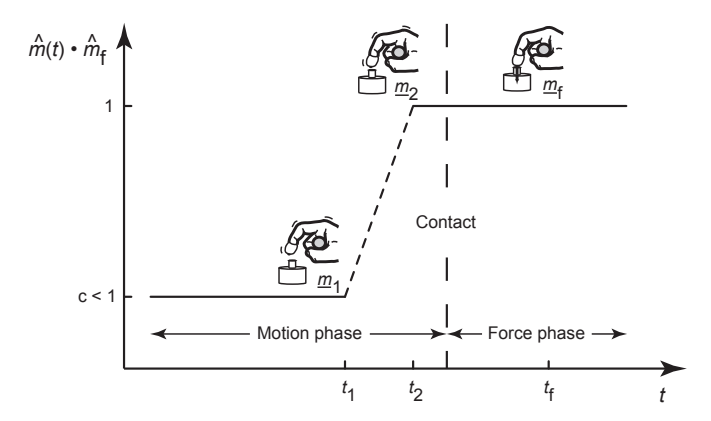


Fig. S2. This figure shows a schematic of the main experimental finding, namely, the muscle coordination pattern vector switches from that for motion to that for static force even before contact occurs. This schematic shows the vector dot product of the unit vector corresponding to the time-varying muscle coordination pattern with the unit vector of the reference muscle coordination pattern. The reference muscle coordination pattern is that which produces static fingertip force. The time-stamps and muscle coordination patterns of interest are indicated using the subscripts 1, 2, and f.

cal between t_1 and t_2 because we found experimentally that the transition happened rapidly (in less than 60ms). Therefore, we make the approximation that $\underline{x}_1 \approx \underline{x}_2$. Leading to, $\Psi(\underline{x}_1) \approx \Psi(\underline{x}_2)$. Call these $\Psi_{\rm m}$ (subscript 'm' for motion). Finally, suppose that \underline{m}_1 , \underline{m}_2 and $\underline{m}_{\rm f}$ are all generated by collinear neural control signals, i.e., there exists \hat{u}^* and scalars k_1 , k_2 , and $k_{\rm f}$ such that

$$\underline{u}_i = k_i \hat{u}^*, i = 1, 2, f$$
 (S4.5)

Substituting these into equation (S3.4) and using appropriate Ψ ,

$$\underline{m}_1 = \Psi_{\mathsf{m}} k_1 \hat{u}^* \tag{S4.6a}$$

$$\underline{m}_2 = \Psi_{\rm m} k_2 \hat{u}^* \tag{S4.6b}$$

$$\underline{m}_{\rm f} = \Psi_{\rm f} k_{\rm f} \hat{u}^* \tag{S4.6c}$$

These relationships are succinctly summarized in Fig. S3.

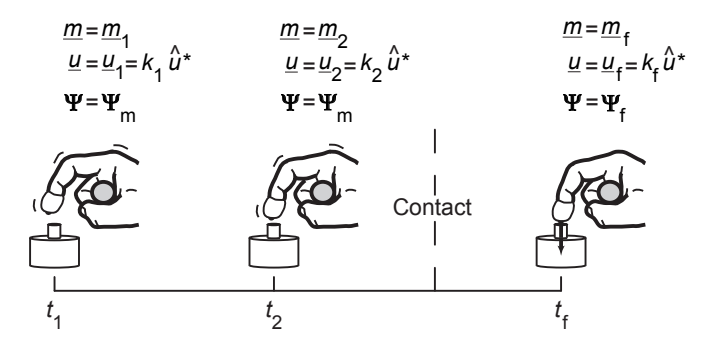


Fig. S3. This figure succinctly summarizes how various relevant variables and mappings change at each snapshot of the finger.

Finally, there are three relationships between muscle coordination patterns that we know to be true based on the experimental results (Fig. S2).

$$\hat{m}_2 \cdot \hat{m}_{\rm f} = 1 \tag{S4.7a}$$

$$\hat{m}_1 \cdot \hat{m}_2 = c \neq 1 \tag{S4.7b}$$

$$\hat{m}_1 \cdot \hat{m}_f = c \neq 1 \tag{S4.7c}$$

These equalities will be used below to show that the underlying neural control signal had to undergo a rapid switch as well.

S4.a Validation of simplified affine model

We first perform a validation of our simplified model to test whether it allows for a change in muscle coordination pattern without a change in the underlying neural control signal. Namely, whether equation (S4.7c) taken by itself can result from collinear underlying neural control signals (equations (S4.6a) - (S4.6c)).

$$\hat{m}_{1} \cdot \hat{m}_{f} \neq 1 \implies \hat{m}_{1} \neq \hat{m}_{f}$$

$$\implies \frac{\cancel{\cancel{N}_{1}} \Psi_{m} \hat{u}^{*}}{\cancel{\cancel{N}_{1}} \|\Psi_{m} \hat{u}^{*}\|} \neq \frac{\cancel{\cancel{N}_{f}} \Psi_{f} \hat{u}^{*}}{\cancel{\cancel{N}_{f}} \|\Psi_{f} \hat{u}^{*}\|}$$

$$\implies \left(\frac{\Psi_{m}}{\|\Psi_{m} \hat{u}^{*}\|} - \frac{\Psi_{f}}{\|\Psi_{f} \hat{u}^{*}\|}\right) \hat{u}^{*} \neq 0$$

$$\hat{u}^{*} \notin \text{null} \left(\frac{\Psi_{m}}{\|\Psi_{m} \hat{u}^{*}\|} - \frac{\Psi_{f}}{\|\Psi_{f} \hat{u}^{*}\|}\right)$$
(S4.8)

It is in general possible to find such a \hat{u}^* that satisfies equation (S4.8) because Ψ_m and Ψ_f are patently different from each other.

S4.b Proof by reductio ad absurdum

Consider the left-hand-side of equation (S4.7b) and substitute for \hat{m}_1 and \hat{m}_2 from equations (S4.6a) and (S4.6a), respectively. This enforces the assumption that the underlying neural

control signals are collinear (i.e., mutually compatible). This assumption leads to the following result.

$$\hat{m}_{1} \cdot \hat{m}_{2} = \frac{\left(\cancel{k}_{1} \Psi_{m} \hat{u}^{*}\right) \cdot \left(\cancel{k}_{2} \Psi_{m} \hat{u}^{*}\right)}{\cancel{k}_{1} \|\Psi_{m} \hat{u}^{*}\| \cancel{k}_{2} \|\Psi_{m} \hat{u}^{*}\|} = 1 \tag{S4.9}$$

This is in direct contradiction with the experimental fact given in equation (S4.7b). Therefore, we can conclude that the motion and force phases of the task are accomplished by mutually incompatible underlying neural control strategies.

S5 Generalizing to include neural and muscle redundancy

S5.a Generalization by considering neural redundancy

Neural redundancy permits changes in the underlying neural control signal that do not reflect as changes in muscle coordination pattern, i.e., relaxing the collinearity assumption of Equation (S4.5). Symbolically stated, there exist $\underline{\epsilon}_1$, $\underline{\epsilon}_2$, and $\underline{\epsilon}_f$ such that,

$$\underline{\epsilon}_1 \in \text{null}(\Psi_{\text{m}})$$
 (S5.10a)

$$\underline{\epsilon}_2 \in \text{null}(\Psi_m)$$
 (S5.10b)

$$\underline{\epsilon}_f \in \text{null}(\Psi_f)$$
 (S5.10c)

leading to,

$$\underline{u}_i = k_i \hat{u}^* + \underline{\epsilon}_i$$
, where $i = 1, 2, f$ (S5.11)

Clearly neural redundancy defined as above has no effect on the proof outlined in Section S4.b so long as $\underline{\epsilon}_i$ are of small enough magnitude for our affine approximation to be reasonable. This is because, by substituting equations (S5.10a) – (S5.10c) in equations (S4.6a) – (S4.6c) it is readily seen that the steps presented in Sections S4.a and S4.b remain exactly unchanged.

S5.b Consideration of muscle redundancy

It remains to be shown that the changes in muscle coordination pattern between t_1 and t_2 were not merely a consequence of muscle redundancy with no effect on joint torques. This result is not immediately apparent because of the following reason. From equation (S3.1) we see that if two muscle coordination patterns \underline{m}_1 and \underline{m}_2 are such that their difference $\underline{m}_1 - \underline{m}_2 \in \text{null}(\mathbf{R})$, then, $\underline{\tau}_1 = \underline{\tau}_2$.

Recall that the moment arm matrix depends only on the posture (Valero-Cuevas et al., 1998, Valero-Cuevas, 2000) and not on the contact with the surface. Therefore the matrix \mathbf{R} at times t_1 , t_2 , and t_f are all nearly identical. This in turn leads to,

$$\hat{m}_2 = \hat{m}_f \implies \hat{\tau}_2 = \hat{\tau}_f$$
 (S5.12a)

Moreover,
$$\hat{\tau}_1 \neq \hat{\tau}_f$$
 cf. Section S2 (S5.12b)

$$\hat{\tau}_1 \neq \hat{\tau}_2$$
 from equations (S5.12a) and (S5.12b)

Hence we conclude the joint torques also switched before contact occurred. Therefore, the observed EMG switch does not reflect an anticipatory transition within the null-space of **R**.

Acknowledgments

We thank Manoj Srinivasan and John Guckenheimer for discussions on the mathematical foundations presented in this note.

References

- Feldman, A., 1986. Once more on the equilibrium-point hypothesis (lambda model) for motor control. J Mot Behav 18 (1), 17–54.
- Gribble, P. L., Ostry, D. J., Sanguineti, V., Laboissiere, R., 1998. Are complex control signals required for human arm movement? Journal of Neurophysiology 79 (3), 1409–1424.
- Ostry, D., Feldman, A., 2003. A critical evaluation of the force control hypothesis in motor control. Experimental Brain Research 153 (3), 275–288.
- Todorov, E., 2000. Direct cortical control of muscle activation in voluntary arm movements: a model. Nature Neuroscience 3, 391–398.
- Valero-Cuevas, F. J., 2000. Predictive modulation of muscle coordination pattern magnitude scales fingertip force magnitude over the voluntary range. J Neurophysiol 83 (3), 1469–79.
- Valero-Cuevas, F. J., Zajac, F. E., Burgar, C. G., 1998. Large index-fingertip forces are produced by subject-independent patterns of muscle excitation. J Biomech 31 (8), 693–703.
- Zajac, F., 1989. Muscle and tendon: properties, models, scaling, and application to biomechanics and motor control. Crit Rev Biomed Eng 17 (4), 359–411.